Biosensors and Bioelectronics 56 (2014) 83–90

Contents lists available at ScienceDirect

Biosensors and Bioelectronics

journal homepage: www.elsevier.com/locate/bios

A label-free electrical impedimetric biosensor for the specific detection of Alzheimer's amyloid-beta oligomers

Jo V. Rushworth [a,*], Asif Ahmed [a], Heledd H. Griffiths [b], Niall M. Pollock [b], Nigel M. Hooper [b], Paul A. Millner [a]

[a] School of Biomedical Sciences, Faculty of Biological Sciences, University of Leeds, Leeds LS2 9JT, UK
[b] School of Molecular and Cellular Biology, Faculty of Biological Sciences, University of Leeds, Leeds LS2 9JT, UK

ARTICLE INFO

Article history:
Received 2 October 2013
Received in revised form
2 December 2013
Accepted 16 December 2013
Available online 24 December 2013

Keywords:
Alzheimer's
Amyloid-beta
Biosensor
Prion
Impedance

ABSTRACT

Alzheimer's disease (AD) is the most common form of dementia, with over 37 million sufferers worldwide and a global cost of over $600 billion. There is currently no cure for AD and no reliable method of diagnosis other than *post-mortem* brain examination. The development of a point-of-care test for AD is an urgent requirement in order to provide earlier diagnosis and, thus, useful therapeutic intervention. Here, we present a novel, label-free impedimetric biosensor for the specific detection of amyloid-beta oligomers (AβO), which are the primary neurotoxic species in AD. AβO have been proposed as the best biomarker for AD and levels of AβO in the blood have been found to correlate with cerebrospinal fluid load. The biorecognition element of our biosensor is a fragment of the cellular prion protein (PrP^C, residues 95–110), a highly expressed synaptic protein which mediates the neuronal binding and toxicity of AβO. During the layer-by-layer sensor construction, biotinylated PrP^C (95–110) was attached *via* a biotin/NeutrAvidin bridge to polymer-functionalised gold screen-printed electrodes. Electrochemical impedance spectroscopy (EIS), cyclic voltammetry and scanning electron microscopy were used to validate biosensor assembly and functionality. EIS was employed for biosensor interrogation in the presence of Aβ oligomers or monomers. The biosensor was specific for the detection of synthetic AβO and gave a linear response, without significant detection of monomeric Aβ, down to an equivalent AβO concentration of ~0.5 pM. The biosensor was also able to detect natural, cell-derived AβO present in conditioned medium. The eventual commercialisation of this biosensor system could allow for the early diagnosis and disease monitoring of AD.

© 2013 Elsevier B.V. All rights reserved.

1. Introduction

Alzheimer's disease (AD) is a worldwide socio-economic crisis with over 37 million sufferers and a global cost of over $600 billion (Wimo and Prince, 2010). The incidence of AD is increasing dramatically due to the ageing population and the lack of a drug which can halt or reverse the disease. It is predicted that one in three people alive today will die with some form of dementia, of which AD is the most common. Although there are certain drugs which can slow down AD progression, they are usually given too late to be effective due to the difficulty in diagnosing AD until after the early clinical stages. Currently, the only way to diagnose AD unequivocally is by *post-mortem* examination of the brain. A diagnostic test for AD in living patients is required urgently as this will allow for quicker and much more effective therapeutic intervention and disease monitoring.

The amyloid-beta (Aβ) peptide is the major causative agent of AD (Hardy, 2006). Aβ is a natural product of low abundance in the healthy brain, where it is cleaved out of the neuronally-expressed amyloid precursor protein (APP) by sequential action of beta and gamma secretase enzymes (Vardy et al., 2005). The Aβ peptide, particularly that of 42 amino acids in length ($Aβ_{1-42}$), accumulates in the AD brain. Aβ is highly aggregation prone and, as it builds up, forms a wide range of soluble assemblies, termed oligomers, which vary in size, morphology and conformation from dimers and trimers up to large globular structures of over 1 MDa in size, finally depositing in insoluble fibrils within senile plaques (Rushworth and Hooper, 2010). Of the monomeric, oligomeric and fibrillar forms of Aβ, a plethora of evidence now indicates that soluble Aβ oligomers (AβO) are the major neurotoxic species in AD. AβO bind to neurons, particularly at the post-synaptic membrane,

Abbreviations: Aβ, amyloid-beta; AβO, amyloid-beta oligomers; AD, Alzheimer's disease; APP, amyloid precursor protein; CSF, cerebro-spinal fluid; EIS, electrochemical impedance spectroscopy; LTP, long-term potentiation; POPA, co-polymer formed from tyramine and 3-(4-hydroxyphenyl) propionic acid; PrP^C, cellular prion protein

* Correspondence to: Level 7 LIGHT Laboratories, University of Leeds, Clarendon Way, Leeds LS2 9JT, UK.
E-mail address: j.v.h.rushworth@leeds.ac.uk (J.V. Rushworth).

0956-5663/$ - see front matter © 2013 Elsevier B.V. All rights reserved.
http://dx.doi.org/10.1016/j.bios.2013.12.036

causing synaptic dysfunction, blocking key processes which underlie memory and learning (e.g. long-term potentiation; LTP) and causing neurotoxicity and cell death at low concentrations (Sakono and Zako, 2010; Um et al., 2012; Walsh et al., 2002; Walsh and Selkoe, 2007). The level of AβOs in the brain, particularly those with a "fibrillar" conformation, correlate with AD onset and severity much more strongly than the insoluble fibrillar load (Lesne et al., 2008; Roychaudhuri et al., 2009; Tomic et al., 2009). Importantly, AβO have been detected in animal models of AD before the phenotypic presentation of disease (Wesson et al., 2010). The development of more sensitive diagnostic tests to detect very low levels of biologically-relevant AβO could ultimately lead to clinically useful tests for pre-symptomatic diagnosis and monitoring of AD progression, either before or during disease onset and throughout therapeutic intervention.

In terms of measuring AβO in a patient, it has been proposed that the AβO count in patient fluids (i.e. blood and cerebro-spinal fluid; CSF) reflects the most direct and relevant biomarker for AD (Wang-Dietrich et al., 2013). Levels of AβO in plasma and CSF samples have been shown, by ELISA and flow cytometry, to be elevated in AD and correlate with Mini-Mental State Examination (MMSE) scores (Santos et al., 2012; Wang-Dietrich et al., 2013; Zhou et al., 2012). However, many ELISA-type assays have not been able to detect AβO in CSF, although AβO were detected in AD brain samples (Yang et al., 2013). Crucially, Kasai and colleagues showed recently that levels of AβO in serum correlate directly with the CSF AβO load, demonstrating that a blood test type assay for AβO is relevant to the AβO content in CSF (Kasai et al., 2013).

Measuring AβO levels in patient fluids by conventional laboratory techniques such as ELISA-type assays is time consuming and expensive. Biosensors offer a much more rapid, cost-effective highly sensitive method of analyte detection at the point-of-care. Several efforts to generate a laboratory-based Aβ biosensor have been made recently (Supplementary Table 1) although none of these systems is specific for AβO due to the nature of the bioreceptors employed. Stravalaci and colleagues sought to develop an SPR-based assay that recognises specifically AβO, however, their use of the pan-Aβ antibody 4G8 as bioreceptor would also recognise other Aβ aggregation states as well as APP and its metabolites in patient samples (Stravalaci et al., 2012). An electrochemical biosensor which utilised a ferrocene-conjugated peptide as bioreceptor was shown recently to detect synthetic AβO down to 240 pM, however there was also some recognition of monomeric Aβ and the system was not tested using biologically relevant species (Li et al., 2012). The fabrication of an AβO-specific biorecognition element will allow for the detection of biologically relevant AβO without detecting any other Aβ assemblies, such as monomers and fibrils, or APP metabolites.

Here, we have exploited the cellular prion protein (PrP^C), which is a natural, neuronal receptor that binds specifically to AβO without significant binding of Aβ monomers or fibrils (Chen et al., 2010; Laurén et al., 2009; Rushworth et al., 2013a). PrP^C is abundantly expressed in the brain where it plays neuroprotective roles and yet is also implicated in AD neuropathology (Griffiths et al., 2011; Whitehouse et al., 2010). Several studies have identified the core AβO binding region on PrP^C as residues 95–110 (amino acid sequence THSQWNKPSKPKTNMK) located within the unstructured N-terminal region of the protein (Chen et al., 2010; Kang et al., 2013; Laurén et al., 2009).

Compared with other assays, electrochemical biosensors offer the key advantages of low cost, small size and ease of operation (Millner et al., 2012). In particular, impedimetric sensors offer reagentless, label-free detection of very small quantities of analyte within complex matrices such as serum (Billah et al., 2008; Caygill et al., 2012), milk (Tsekenis et al., 2008) and urine (Pan et al., 2010).

Here, a label-free impedimetric biosensor, which employed a synthetic peptide comprising of PrP^C residues 95–110 as bioreceptor, was constructed upon screen-printed gold electrodes. The gold electrodes were functionalised with a novel co-polymer, derived from a mixture of tyramine and its carboxylic acid analogue, 3-(4-hydroxyphenyl) propionic acid. Biotinylated PrP^C(95–110) peptide was tethered to the polymer-coated electrodes *via* the high-affinity biotin/NeutrAvidin interaction. The sensor construction was verified electrochemically, and through on-sensor blotting and scanning electron microscopy (SEM), before interrogation using electrochemical impedance spectroscopy (EIS) following incubation in the presence of AβO or Aβ monomer. This sensor was found to be specific for AβO, without binding monomeric Aβ, and could detect AβO down to an equivalent concentration of ~0.5 pM. Finally, the biosensor was validated using natural, cell-derived Aβ oligomers that are similar in nature to those found in the cerebro-spinal fluid of AD patients.

2. Materials and methods

2.1. Materials

Custom screen-printed gold electrodes (CX2223AT) were supplied by DropSens S.L. (Oviedo, Spain). Custom synthesised, lyophilised biotin-LC-PrP^C (residues 95–110; THSKWNKPSKPKTNMK) was purchased from Peptide Protein Research Ltd., Fareham, UK. Unlabelled $A\beta_{1-42}$ and biotin-LC-$A\beta_{1-42}$ (both human sequences) were obtained from AnaSpec (San Jose, USA). In the synthetic peptides, LC represents an aminohexanoic acid linker to provide space between the peptide and the biotin moiety. Horseradish peroxidase-conjugated streptavidin (HRP-streptavidin), 1-ethyl-3-(3-dimethylaminopropyl) carbodiimide (EDC) and enhanced chemiluminescence (ECL) reagent were from Thermo Fisher Scientific (Northumberland, UK). HRP-conjugated anti-rabbit and anti-sheep antibodies were from Sigma-Aldrich (Dorset, UK). Anti-*S. pyogenes* polyclonal antibody was raised in a rabbit host against heat-inactivated *S. pyogenes* (Genescript; NJ, USA). 6E10 antibody (anti-Aβ1-16) was from Cambridge Bioscience Ltd. (Cambridge, UK). 7PA2 cells were kindly provided by Dr John Boyle (University of Leeds).

All other laboratory chemicals, including tyramine, 3-(4-hydroxyphenyl) propionic acid, sulfosuccinimidyl 4-[*N*-maleimidomethyl]cyclohexane-1-carboxylate (sulfo-SMCC) and (+)-biotin N-hydroxysuccinimide ester (NHS-biotin) were purchased from Sigma-Aldrich (Dorset, UK) and were of analytical grade.

2.2. Methods

2.2.1. Aβ preparation

Monomeric and oligomeric $A\beta_{1-42}$ preparations were as described previously (Laurén et al., 2009; Rushworth et al., 2013a). Briefly, lyophilised Aβ peptide was dissolved to 1 mM in DMSO and then F12 medium added to give a total Aβ peptide concentration of 100 μM. Monomeric Aβ (Aβm) was taken at this point, whereas oligomers (AβO) were formed by incubating the solution for 16 h at room temperature with a final centrifugation step at 14,000 × *g* for 15 min to remove any insoluble aggregates.

2.2.2. Electropolymerisation

Electrodes were immersed in 100% ethanol and subjected to sonication in a water bath for 5 min to remove any dielectric material upon the sensor surface prior to electropolymerisation. Electropolymerisation was carried out using GPES software on an AUTOLAB type III electrochemical workstation (Metrohm Autolab B.V.; Utrecht, Netherlands). To deposit a co-polymer of polytyramine/3-(4-hydroxyphenyl) propionic acid (POPA), electrodes

were immersed in methanol containing 18.75 mM tyramine, 6.25 mM 3-(4-hydroxyphenyl) propionic acid and 0.3 M NaOH. The potential was cycled twice from 0 V to 1.6 V and back to 0 V at a scan rate of 200 mV/s. Following electropolymerisation, electrodes were rinsed in dH_2O and blow-dried gently in a stream of argon.

2.2.3. Attachment of bioreceptors

Polymer-coated electrodes were first equilibrated in PBS for 30 min. For the attachment of biotin-LC-PrP^C (95–110), electrodes were first incubated in the presence of NHS-biotin (1 mg ml^{-1}), followed by NeutrAvidin (1 μM) and finally biotin-LC-PrP^C (95–110) (1 mg ml^{-1}), each for 30 min in PBS with washing steps in between. Sensors were rinsed in dH_2O and blow dried in argon prior to use.

2.2.4. Electrochemical impedance spectroscopy

At each stage of biosensor assembly, and to monitor analyte binding, electrochemical impedance spectroscopy (EIS) was conducted using FRA software on an AUTOLAB type III electrochemical workstation (Metrohm Autolab B.V.; Utrecht, The Netherlands). For analyte testing, fully fabricated biosensors (comprising of biotinylated PrP^C (95–110) peptide tethered *via* biotin-NeutrAvidin to POPA co-polymer-coated DropSens gold electrodes) were subjected to successive incubations first in vector alone as a pre-equilibration step (i.e. DMSO/F12 medium without Aβ) and then in the presence of $Aβ_{1-42}$ monomer or oligomers (total peptide concentration 10^{-12}, 10^{-10}, 10^{-8}, 10^{-6} M), for 20 min at each concentration. After rinsing in dH_2O, the EIS response was recorded for each concentration by immersing the sensors in an electron mediator solution of 10 mM $K_3[Fe(CN)_6]/K_4[Fe(CN)_6]$ (1:1 ratio) in 10 mM PBS, pH 7. For testing of 7PA2 conditioned medium, sensors were pre-equilibrated in blank medium and then incubated for 20 min in the presence of conditioned medium prior to EIS measurements. The impedance analysis was performed over a range of frequencies from 0.25 Hz to 25 kHz, using a modulation voltage of 10 mV at an applied voltage of 0 V versus an Ag/AgCl reference. The R_{ct} (charge-transfer resistance) of the sensor following incubation with Aβ was expressed as a percentage of the R_{ct} of the vector pre-equilibrated sensor.

2.2.5. Cyclic voltammetry

Cyclic voltammetry (CV) was performed in electron mediator solution, comprising of 10 mM $K_3[Fe(CN)_6]/K_4[Fe(CN)_6]$ (1:1 ratio) in 10 mM PBS, pH 7. Two scans were conducted at a rate of 50 mV s^{-1} where the potential was cycled from −0.3 to +0.7 V.

2.2.6. On-sensor chemiluminescent blotting

To verify the selective binding of AβO to the sensor surface, and not Aβ monomer, full sensors were incubated with successive concentrations of either AβO or Aβ monomer as described in Section 2.2.4. Sensors were rinsed in dH_2O and then incubated in the presence of 6E10 antibody (1:5000; anti-Aβ N-terminus), pipetted onto the working electrodes, for 30 min in a moist chamber. After three washes in PBS, rinsing in dH_2O and drying in argon, the electrodes were incubated with HRP-conjugated rabbit anti-mouse secondary antibody (1:5000) as before. Sensors were washed three times for 5 min each in PBS, once in PBS containing 0.1% (v/v) Tween-20 to aid removal of non-specific binding, with a final wash in PBS. Finally, ECL reagent was pipetted onto the working electrodes and chemiluminescence was detected using a G:BOX Gel Imaging System (Syngene Ltd.; Cambridge, UK). Images presented are chemiluminescence only (white light on a black background) and a superimposition of chemiluminescence signal upon the bright field image of the electrodes, where chemiluminescence has been false coloured green to aid viewing.

2.2.7. Cell culture and collection of conditioned medium

7PA2 Chinese hamster ovary (CHO) cells, expressing human APP bearing the V717F familial AD mutation, were kindly provided by Dr John Boyle (University of Leeds) and were as described previously (Podlisny et al., 1995; Shankar et al., 2007). The cells were cultured routinely in Dulbecco's modified Eagle's medium (DMEM) supplemented with 10% (v/v) foetal bovine serum (FBS), 0.024 mg/ml proline, 200 μg/ml G418 Sigma-Aldrich (Dorset, UK) 50 U/ml Penicillin and 0.1 mg/ml streptomycin (Lonza, UK). Cells were maintained in a humidified incubator at 37 °C in a 5% CO_2/95% air atmosphere. For the collection of conditioned medium, cells were grown in a 6-well plate to ~95% confluence, rinsed in serum-free OptiMEM and then incubated in 1 ml of serum-free OptiMEM in the presence or absence of the BACE1 inhibitor βIV (10 μM) for 24 h. The OptiMEM was harvested, centrifuged at 14,000 × *g* to remove cellular debris and then stored at −20 °C until use.

3. Results

3.1. Electrochemical confirmation of layer-by-layer biosensor surface assembly

A schematic diagram showing the biosensor architecture is presented in Fig. 1A. A layer-by-layer sensor construction approach

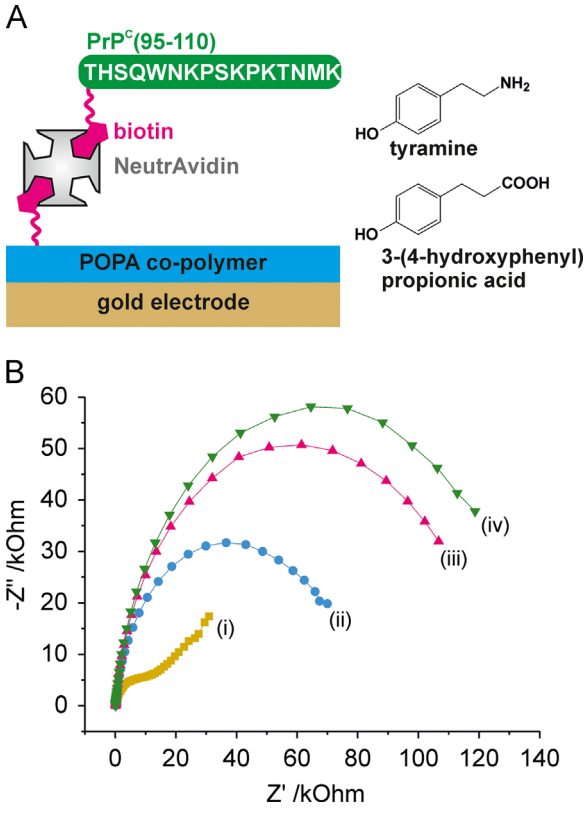

Fig. 1. Layer-by-layer biosensor construction verified by impedance spectroscopy (A) Gold electrodes were coated in POPA (polytyramine/poly 3-(4-hydroxyphenyl propionic acid)) by electropolymerisation. The pendant amine groups presented by the tyramine moieties were functionalised with NHS-biotin, followed by the addition of NeutrAvidin, which permitted the high-affinity (K_d ~ 10^{-15} M) attachment of biotinylated PrP^C(95–110) as bioreceptor. Chemical structures of tyramine and 3-(4-hydroxyphenyl) propionic acid utilised in the POPA co-polymer. (B) Biosensors were analysed by EIS at each stage of construction; Nyquist plots of impedance show (i) bare gold, (ii) POPA co-polymer, (iii) biotin/NeutrAvidin and (iv) full sensor with biotin-LC-PrP^C(95–110) attached. Impedance spectra were recorded in a solution of PBS, pH 7.0, containing 10 mM $Fe(CN)_6^{3-/4-}$ over a frequency range of 25 kHz–0.25 Hz. The imaginary component of impedance (|Z''|) is plotted against the real component of impedance (Z').

was employed here, whereby biotinylated PrP^C peptide (residues 95–110) was tethered to polymer-coated DropSens gold electrodes *via* the high affinity ($K_d \sim 10^{-15}$ M) biotin-NeutrAvidin linkage. This was achieved by first cleaning the gold electrodes by sonication and then by successive incubations in the presence of the appropriate reagents, with washing steps in between, as detailed in Section 2.2.

Electrochemical impedance spectroscopy (EIS) is a very powerful tool for the characterisation of surface interfaces and for the detection of very small changes occurring at biosensor surfaces. EIS is widely used in electrochemical biosensing both as readout for analyte binding and as a confirmatory technique to validate the layer-by layer deposition of materials upon a sensor surface.

Here, the assembly of each layer of the biosensor surface was confirmed by EIS. Impedance measurements were carried out in 10 mM $Fe(CN)_6^{3-/4-}$ over a range of frequencies from 25 kHz down to 0.25 Hz. The resulting complex impedance data are displayed as a Nyquist plot in Fig. 1B, where the imaginary component of impedance (|Z″|, related to capacitance) is displayed as a function of the real component of impedance (Z′, related to resistance). These impedance spectra are typical of the theoretical, semi-circular shape observed when the data are modelled using a Randles′ equivalent circuit, a useful tool in interpreting EIS data which accounts for the resistive and capacitative processes which occur at different frequencies. The semi-circular Nyquist plots increased in size as sequential material, namely polymer, NHS-biotin/NeutrAvidin and bioreceptor, was incubated upon the gold sensor surface. This is a good indication of successful layer-by-layer biosensor construction, as increasing material provided a larger charge-transfer resistance (semi-circle diameter, Z′) which indicated a greater blocking effect between the redox probe and the biosensor surface.

3.2. Polymer characterisation by cyclic voltammetry, impedance spectroscopy and scanning electron microscopy (SEM)

The co-polymer employed here, which we have termed "POPA", was electrodeposited from a 3:1 M ratio of tyramine and 3-(4-hydroxyphenyl) propionic acid in methanol containing 0.3 M NaOH as dopant (see Fig. 1A for chemical structures). Poly(tyramine) has been employed previously in impedimetric biosensor construction as a stable, non-conducting polymer which presents pendant amine groups for surface bio-functionalisation (Pournaras et al., 2008). Here, the carboxylic acid analogue of tyramine, 3-(4-hydroxyphenyl) propionic acid, was also included in the polymer in order to provide more favourable spacing of pendant amine groups and to incorporate negative charge into the biosensor surface, aiming to minimise non-specific binding of biomolecules.

The characterisation of POPA is shown in Fig. 2. Cyclic voltammetry (CV) plots, obtained during the process of electropolymerisation, demonstrated that the electrodeposition profile of POPA is similar to that of polytyramine (Fig. 2A and B). Impedance spectra were then obtained for these polymer-coated electrodes, as described above, and displayed as Nyquist plots (Fig. 2C). For POPA, the maximum height of the semi-circle (i.e. C_{dl}, double-layer capacitance) and the maximum diameter of the semi-circle (i.e. R_{ct}, charge-transfer resistance) were approximately half of the corresponding values observed for polytyramine. This may be advantageous because full sensors constructed upon polytyramine become too capacitative, leading to a loss of data at the low-frequency end of the Nyquist plot (data not shown). In contrast, POPA-based sensors generate a full semi circular Nyquist plot which allows for more accurate determination of R_{ct} values.

Scanning electron microscopy (SEM) confirmed the deposition of a layer of porous material upon the gold working electrodes following electrodeposition of POPA (Fig. 2D and E). Taken together, these data indicate that the novel co-polymer, POPA, is electrodeposited onto gold electrodes where it provides a relatively low starting impedance for the construction of biosensors.

3.3. Detection of analyte recognition by impedance spectroscopy

Initially, biosensors were calibrated using synthetic AβO prepared in tissue culture medium. AβO can be highly heterogeneous and vary greatly in size and conformation (Rushworth and Hooper, 2010). Therefore, it was important to prepare stable and biologically relevant AβO. Soluble AβO with a particular "fibrillar" surface epitope (as evidenced by immunoreactivity with the anti-fibrillar antibody, OC) correlate best with AD onset and severity, and are likely to represent the major neurotoxic species in the AD brain (Kayed et al., 2007; Tomic et al., 2009). Here, we prepared soluble, fibrillar AβO from synthetic $A\beta_{1-42}$ peptide as described previously (Chromy et al., 2003; Laurén et al., 2009; Rushworth et al., 2013a). We have demonstrated previously that these oligomers are free from fibrils and present a fibrillar conformation, as evidenced by their reactivity with the OC antibody (Rushworth et al., 2013a). Biosensors were first equilibrated in vector only (i.e. the DMSO/F12 medium in which the AβO were prepared) and then incubated in the presence of successive concentrations of AβO (total peptide concentration from 10^{-12} to 10^{-6} M) for 20 min per incubation, followed by rinsing in dH_2O and immersion in 10 mM $Fe(CN)_{6(aq)}^{3-/4-}$ redox mediator solution for EIS measurements. The EIS data from a representative sensor are presented as Nyquist plots in Fig. 3. A decrease in impedance was observed with increasing AβO concentration, as evidenced by the decreasing height and diameter of the semi-circular Nyquist traces, which correspond to decreased capacitance and resistance of the sensor surface respectively.

The fitting of the Nyquist plot data presented in Fig. 3 to the Randles′ equivalent circuit model generated the EIS parameters R_s (solution resistance), R_{ct} (charge-transfer resistance) and *CPE* (constant phase element, an equivalent model of double-layer capacitance), which are presented in Table 1. Good stability of the sensor was observed as the solution resistance was constant at all stages of biosensor construction and testing. Whilst the R_{ct} values decreased upon addition of AβO, showing a clear trend, the *CPE* values were slightly variable and did not indicate any trend. Therefore, as the system is based on Faradic impedance, measured in presence of redox mediators, R_{ct} was chosen as the parameter to evaluate the binding of AβO and Aβ monomer to the sensors in subsequent experiments.

Often, the binding of analyte to a biosensor surface causes an increase in impedance, and this has been widely reported (Millner et al., 2012). An increase in impedance is typically due to the increasing deposition of a substance upon the sensor surface which increases the capacitance and resistance of that surface. However, although less widely reported, the binding of certain analytes to certain biosensor systems can decrease the impedance of the surface (Zhang et al., 2012). The Aβ peptide binds to various metal cations including Cu^{2+}, Zn^{2+} and Fe^{3+} which are present in the buffer solutions used here (Nair et al., 2010). The binding of the metal ion-complexed amyloid protein tau to a functionalised biosensor surface has been shown electrochemically to increase the current density through the surface (Martic et al., 2013).

We wished to verify that the binding of AβO to the biosensor caused a decrease in impedance by increasing current flow through the surface. To do this, biotin-labelled AβO were prepared as described previously for unlabelled peptide. Biosensors were constructed up to the level of NeutrAvidin and then incubated in the presence of biotinylated AβO for 20 min prior to EIS measurements (Fig. 4A). As a control for normal sensor response, other sensors were incubated in the presence of biotinylated antibody which is known to increase the impedance of the sensor surface

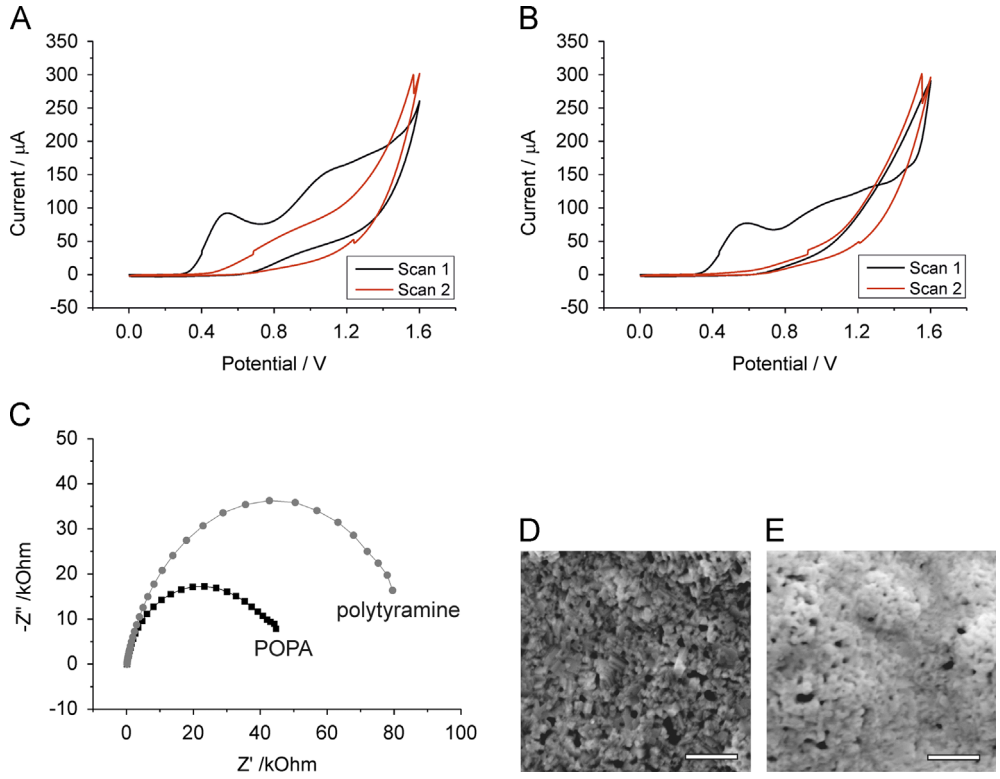

Fig. 2. Characterisation of the co-polymer POPA. The electropolymerisation of either (A) polytyramine from a 25 mM solution of tyramine or (B) POPA from a 3:1 M ratio of tyramine (18.25 mM) and 3-(4-hydrozyphenyl) propionic acid (6.75 mM), both in methanol containing 0.3 M NaOH, was conducted using cyclic voltammetry (CV), as described in Section 2.2. (C) EIS measurements obtained in 10 mM $Fe(CN)_{6(aq)}^{3-/4-}$ in PBS for polytyramine and POPA that were deposited in A and B, respectively. Scanning electron microscopy (SEM) was employed to compare the surface of a gold working electrode (D) before and (E) after electropolymerisation of POPA. Scale bar, 500 nm.

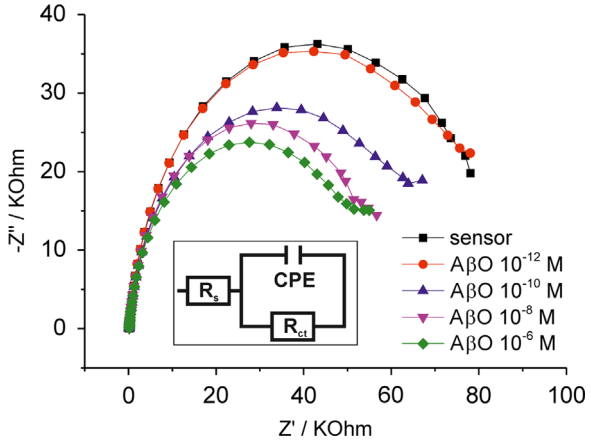

Fig. 3. Biosensor response to Aβ oligomers as measured by EIS. The response of the biosensors to AβO was analysed by EIS. Following equilibration in vector solution alone (sensor), cumulative additions of AβO (10^{-12}–10^{-6} M total Aβ peptide concentration) were performed for 20 min each prior to rinsing and EIS measurement in a solution of PBS containing 10 mM $Fe(CN)_{6(aq)}^{3-/4-}$. Inset shows the Randles' equivalent circuit model for this system where R_s = solution resistance, R_{ct} = charge-transfer resistance and *CPE* = constant phase element, a model of an imperfect double layer capacitor.

(Fig. 4B). The attachment of the biotinylated AβO to the NeutrAvidin functionalised surface caused a decrease in impedance, whereas the binding of biotinylated antibody caused the expected increase in impedance. Following incubation of the sensor with AβO, the current flow through the surface was measured using cyclic voltammetry (Fig. 4C). The CV trace becomes broader upon the addition of biotinylated AβO to the NeutrAvidin-coated surface,

Table 1
Values for the EIS parameters obtained from fitting the Nyquist plots shown in Fig. 3 to the Randles' circuit.

Electrode	R_s (Ω)	R_{ct} (kΩ)	*CPE* (nF)
POPA-coated gold	161	60.1	241
Full sensor	160	86.7	268
AβO 1 pM	157	85.9	242
AβO 100 pM	153	71.4	170
AβO 10 nM	169	59.0	456
AβO 1 μM	158	57.1	279

indicating that the binding of AβO increases the conductivity of the surface, which corroborates the observed decrease in impedance.

3.4. Calibration curves of Aβ oligomer and Aβ monomer recognition

In order to obtain calibration curves, multiple sensors ($n=6$) were incubated in the presence of either AβO or Aβ monomer, as detailed previously in Section 3.3. The charge-transfer resistance (R_{ct}, or diameter of the Nyquist plot from the Z′ axis) for each analyte concentration was calculated by fitting semi-circles to the Nyquist traces using FRA software on an AUTOLAB station. The R_{ct} values obtained after each incubation with Aβ were expressed as a percentage of the R_{ct} value obtained from the vector-equilibrated sensor (Fig. 5). The sensor demonstrated an inverse relationship between the change in R_{ct} and AβO concentration and showed specificity for AβO down to a total Aβ concentration of 10^{-10} M (or 100 pM). Previous studies indicate that each oligomeric Aβ assembly likely contains approximately 100 monomers, and that approximately half of the oligomer preparation remains monomeric (Fluharty et al., 2013; Laurén et al., 2009), so this sensor can likely discriminate Aβ oligomers at a true oligomer concentration

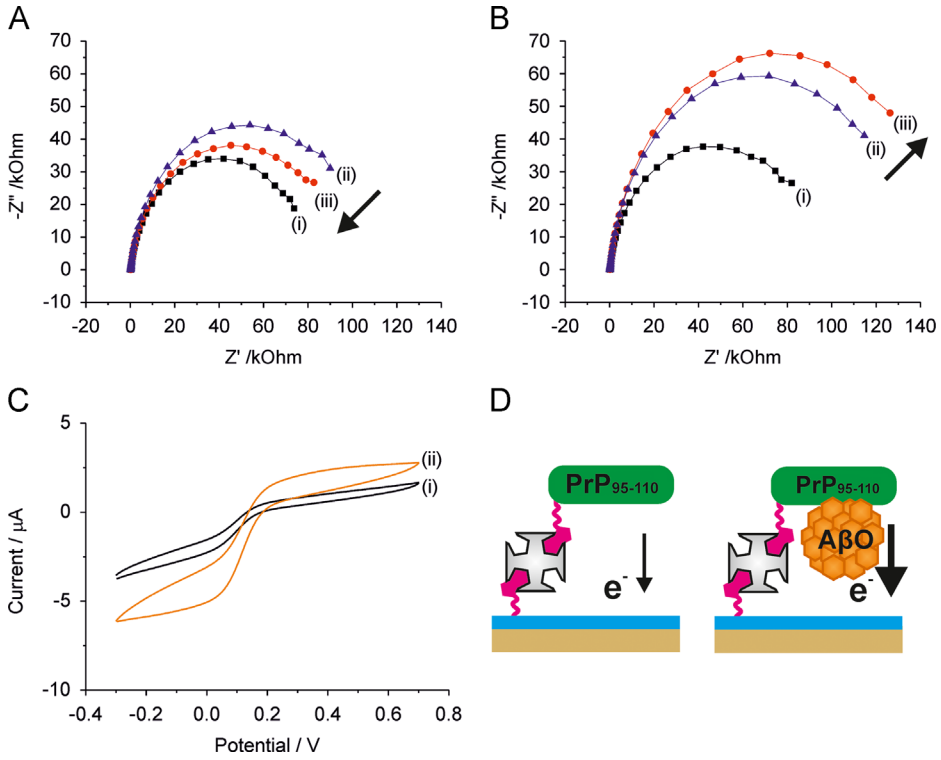

Fig. 4. Electrochemical investigation of the effect of Aβ oligomers upon the conductivity of the sensor surface. Sensors constructed up to the level of NeutrAvidin were incubated in the presence of (A) biotinylated AβO or (B) biotinylated anti-*Streptococcus pyogenes* antibody as analyte, both at a concentration of 10^{-6} M for 20 min. EIS measurements were taken at the level of (i) polymer, (ii) biotin/NeutrAvidin and (iii) after incubation with biotinylated analyte. (C) Analysis of the sensor in A by cyclic voltammetry (CV) (i) at the level of biotin/NeutrAvidin and (ii) after incubation with biotinylated Aβ oligomers. CV analysis performed by cycling the potential twice between −0.3 and +0.7 V at a scan rate of 50 mV s^{-1} in a solution of PBS containing 10 mM $Fe(CN)_{6(aq)}^{3-/4-}$. (D) A schematic diagram indicating an increase in surface conductivity in the presence of bound Aβ oligomers.

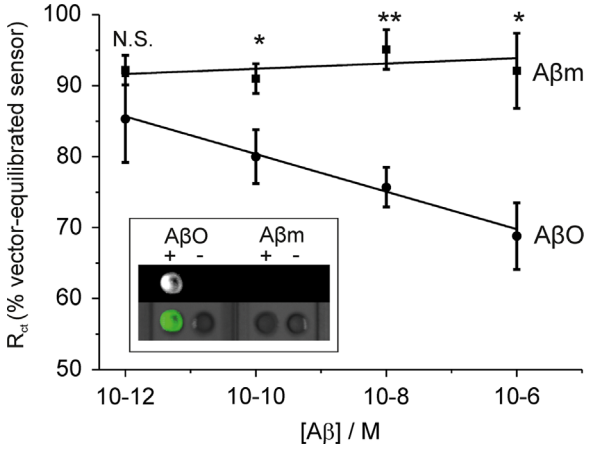

Fig. 5. Calibration curves of Aβ oligomer and Aβ monomer binding. The response of multiple biosensors to cumulative incubation in the presence of either (i) AβO or (ii) fresh, monomeric Aβ peptide was determined by EIS, as described in Fig. 4. The R_{ct} value following incubation with Aβ, expressed as a percentage of the vector-equilibrated sensor R_{ct} value, was determined from the Nyquist plots using FRA software on an AUTOLAB station. Graph shows mean of $n=6 \pm$ SEM. These % R_{ct} values was compared statistically for Aβ monomer and AβO using the Mann–Whitney-U test; **, $p<0.01$; *, $p<0.05$; N.S., $p>0.05$. Inset figure shows chemiluminescent blotting of biosensors after EIS testing in the presence (+) or absence (−) of anti-Aβ 6E10 antibody, followed by HRP-conjugated secondary antibody, to detect any bound Aβ (monomeric or oligomeric). Top panel shows chemiluminescence only; bottom panel shows chemiluminescence, false coloured green to aid viewing, overlaid onto the electrodes.

of ~0.5 pM. The reproducibility of the electrodes was good, with there being a linear fit (Pearson's r value = −0.991) between the R_{ct} values obtained with AβO testing (Fig. 5). This is likely due in part to the screen-printed electrodes employed here, of which the batch fabrication method gives reduced electrode-to-electrode variability compared with other systems (Rushworth et al., 2013b).

To confirm the specificity of the biosensor for binding AβO and not monomer, on-sensor chemiluminescent blotting was employed (Rushworth et al., submitted). After the final incubation in the presence of AβO or monomers (10^{-6} M), sensors were rinsed extensively in dH_2O, dried in argon and incubated in the presence of the pan-Aβ murine antibody 6E10 (1:5000 for 30 min in PBS). After extensive washing in PBS, the sensors were incubated with HRP-conjugated rabbit anti-mouse secondary antibody as before. After washing in PBS and PBS containing 0.1% Tween-20 to reduce non-specific binding, ECL reagent was pipetted onto the working electrodes which were imaged to detect a chemiluminescent signal (Fig. 5). A strong chemiluminescent signal was observed where the sensors had been exposed to AβO, but not Aβ monomers, with no binding of the secondary antibody alone. These data corroborate the specificity of the biosensor for AβO and not monomer.

3.5. Validation of the biosensor using natural, cell-derived Aβ oligomers

Finally, we tested the ability of the sensor to recognise biologically relevant AβO. A well known cellular model of Aβ oligomers is the Chinese hamster ovary (CHO) cell line termed 7PA2 which stably expresses human APP bearing the Val717Phe familial AD mutation (Podlisny et al., 1998; Walsh et al., 2002). These cells secrete natural AβO which have been shown to block LTP, disrupt memory and learning and cause neurotoxicity in vitro and in vivo (Cleary et al., 2005; Poling et al., 2008; Shankar et al., 2007; Wang et al., 2004). These oligomers are similar to those found in the cerebro-spinal fluid of AD patients (Shankar et al., 2008; Walsh and Selkoe, 2007).

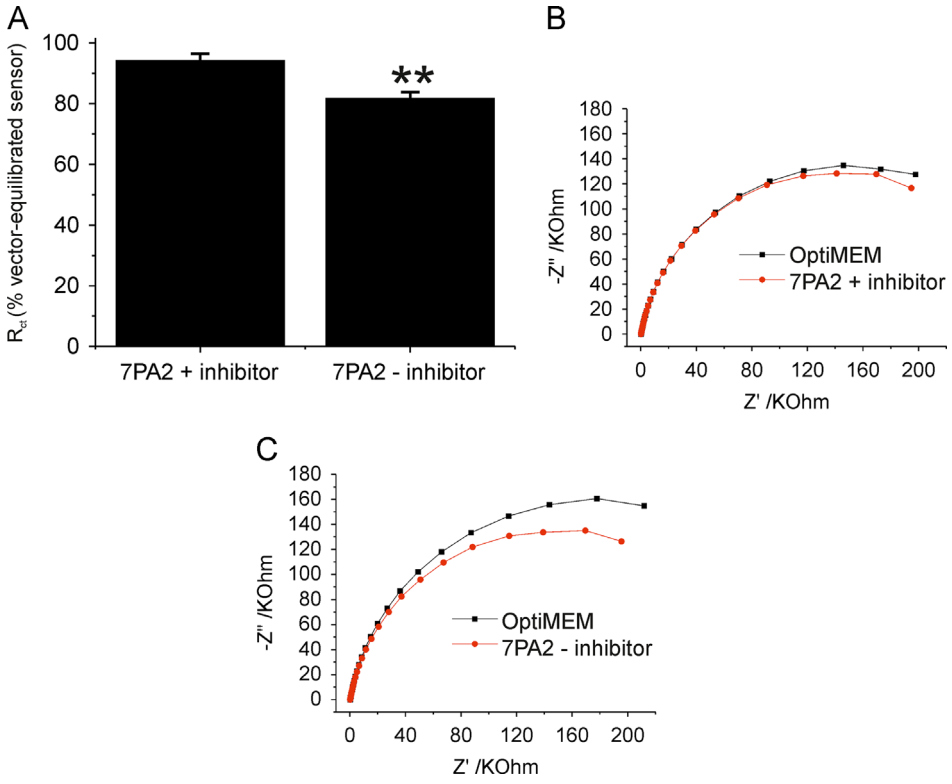

Fig. 6. Biosensor response to cell-derived, natural Aβ oligomers. (A) Full sensors were incubated for 20 min with medium alone and subsequently in the presence of conditioned medium (CM) derived from 7PA2 CHO cells that had been cultured in the presence or absence of the BACE1 inhibitor βIV. Impedance measurements were presented as Nyquist plots and then the R_{ct} of the sensor after incubation with 7PA2 CM was expressed as a percentage of the R_{ct} of the OptiMEM-equilibrated sensor. Graph shows mean of $n=3\pm$ SEM, **, $p=0.008$. B and C show representative Nyquist plots obtained from biosensors incubated in the presence of 7PA2 medium which had been obtained either (B) in the presence or (C) in the absence of BACE1 inhibitor.

Furthermore, the neurotoxicity of these natural AβO is transduced through PrP^C (Bate and Williams, 2011; Resenberger et al., 2011). To evaluate the ability of our PrP^C-based biosensor to recognise cell-derived AβO, we harvested conditioned medium from 7PA2 CHO cells which had been cultured in OptiMEM in the presence or absence of the beta-secretase inhibitor βIV which prevents the generation of Aβ through inhibition of the APP processing enzyme BACE1. The conditioned medium was centrifuged to remove any cellular debris before incubation with the biosensor. In the same manner as before, sensors were pre-equilibrated in OptiMEM alone and then incubated in the presence of 7PA2 conditioned medium (Fig. 6).

In the presence of the AβO-containing 7PA2 conditioned medium, a decrease in R_{ct} of 18.2% was observed, indicating a decrease in impedance. When the BACE1 inhibitor was present, the decrease was much smaller at 5.8%. These data indicate that the biosensor is able to detect natural Aβ oligomers in biologically relevant cell medium. Typically, Aβ oligomers are reported to be present in 7PA2 CHO medium at a concentration of approximately 1–2 nM (Bate and Williams, 2011; Podlisny et al., 1995). Using the equation of the line of best fit shown for the AβO in Fig. 6, the concentration of AβO in the 7PA2 conditioned medium sample was calculated to be 24.0 nM.

4. Conclusions and future perspectives

In this study, a novel biosensor for the specific and sensitive detection of AβO is presented. The sensor has the significant advantages of being (i) label-free, allowing for the detection of natural oligomers and (ii) specific for AβO due to the use of the synthetic non-antibody PrP^C fragment as bioreceptor, instead of a pan-Aβ antibody which recognises other species. Our data indicate that the sensor is able to discriminate between synthetic AβO and Aβ monomer at an Aβ concentration of 100 pM, which likely relates to an AβO concentration of around 0.5 pM. The specificity of the sensor for AβO binding was confirmed by on-sensor chemiluminescent blotting, which did not detect any Aβ monomer binding to the sensor. Importantly, the sensor was shown to function in conditioned medium to facilitate the detection of natural AβO secreted by a human APP-expressing cell line. This is a good indication that the sensor could operate in biological fluids such as CSF and blood, as no processing of the sample was carried out other than a brief centrifugation step and the conditioned cell medium employed is a complex medium, comparable to serum or CSF, containing trace amounts of serum as well as various proteins, amino acids and cell metabolites. Compared to previous biosensor systems for the detection of AβOs (Supplementary Table 1), our system is exquisitely sensitive, highly specific for AβOs and facilitates detection of biologically-relevant species in a complex matrix. Future work would seek to validate the biosensor in patient fluids obtained from AD and age-matched control patients. There is also scope to improve further the sensitivity and specificity of the sensor, for example by investigating other PrP peptides and by modifying the length of the linker between polymer and bioreceptor. Importantly, reproducibility of the system must be optimised in order that this laboratory-based system can be translated into a commercial device. In order to increase the reproducibility of the sensors, electrode fabrication methods need to be improved and the use of robotics employed in sensor fabrication in order to minimise variability of the starting electrodes and the final sensors. To our knowledge, this is the first time that a co-polymer has been generated from a mixed solution of tyramine and 3-(4-hydroxyphenyl) propionic acid. This novel co-polymer, which we have

termed POPA, merits further investigation as it appears to be stable, generates a consistent layer on the electrode surface and demonstrates low non-specific binding of Aβ monomer.

Acknowledgements

The authors are grateful to the Alzheimer's Research UK (PG2010-2) for funding. AA was funded by a Fully-Funded International Research Scholarship (FIRS, University of Leeds). We thank Dr John Boyle for kindly providing the 7PA2 cells and Martin Fuller for SEM training and helpful advice. We are also grateful to Jack Goode for helpful electrochemical discussions.

Appendix A. Supplementary material

Supplementary data associated with this article can be found in the online version at http://dx.doi.org/10.1016/j.bios.2013.12.036.

References

Bate, C., Williams, A., 2011. J. Biol. Chem.
Billah, M., Hays, H.C.W., Millner, P.A., 2008. Microchim. Acta 160, 447–454.
Caygill, R.L., Hodges, C.S., Holmes, J.L., Higson, S.P., Blair, G.E., Millner, P.A., 2012. Biosens. Bioelectron. 32, 104–110.
Chen, S., Yadav, S.P., Surewicz, W.K., 2010. J. Biol. Chem. 285, 26377–26383.
Chromy, B.A., Nowak, R.J., Lambert, M.P., Viola, K.L., Chang, L., Velasco, P.T., Jones, B. W., Fernandez, S.J., Lacor, P.N., Horowitz, P., et al., 2003. Biochemistry 42, 12749–12760.
Cleary, J.P., Walsh, D.M., Hofmeister, J.J., Shankar, G.M., Kuskowski, M.A., Selkoe, D.J., Ashe, K.H., 2005. Nat. Neurosci. 8, 79–84.
Fluharty, B.R., Biasini, E., Stravalaci, M., Sclip, A., Diomede, L., Balducci, C., La Vitola, P., Messa, M., Colombo, L., Forloni, G., et al., 2013. J. Biol. Chem. 288, 7857–7866.
Griffiths, H.H., Whitehouse, I.J., Baybutt, H., Brown, D., Kellett, K.A., Jackson, C.D., Turner, A.J., Piccardo, P., Manson, J.C., Hooper, N.M., 2011. J. Biol. Chem.
Hardy, J., 2006. J. Alzheimer's Dis. 9, 151–153.
Kang, M., Kim, S.Y., An, S.S., Ju, Y.R., 2013. Exp. Mol. Med. 45, e34.
Kasai, T., Tokuda, T., Taylor, M., Kondo, M., Mann, D.M.A., Nakagawa, M., Allsop, D., 2013. Neurosci. Lett. , http://dx.doi.org/10.1016/j.neulet.2013.06.029.
Kayed, R., Head, E., Sarsoza, F., Saing, T., Cotman, C.W., Necula, M., Margol, L., Wu, J., Breydo, L., Thompson, J.L., et al., 2007. Mol. Neurodegener. 2, 18.
Laurén, J., Gimbel, D.A., Nygaard, H.B., Gilbert, J.W., Strittmatter, S.M., 2009. Nature 457, 1128–1132.
Lesne, S., Kotilinek, L., Ashe, K.H., 2008. Neuroscience 151, 745–749.
Li, H., Cao, Y., Wu, X., Ye, Z., Li, G., 2012. Talanta 93, 358–363.
Martic, S., Rains, M.K., Kraatz, H.B., 2013. Anal. Biochem..
Millner, P.A., Caygill, R.L., Conroy, D.J., Shahidan, M.A., 2012. Impedance interrogated affinity biosensors for medical applications: novel targets and mechanistic studies, Vol 45. Woodhead Publishing Ltd., Cambridge, UK.
Nair, N.G., Perry, G., Smith, M.A., Reddy, V.P., 2010. J. Alzheimers Dis. 20, 57–66.
Pan, Y., Sonn, G.A., Sin, M.L.Y., Mach, K.E., Shih, M.C., Gau, V., Wong, P.K., Liao, J.C., 2010. Biosens. Bioelectron. 26, 649–654.
Podlisny, M.B., Ostaszewski, B.L., Squazzo, S.L., Koo, E.H., Rydell, R.E., Teplow, D.B., Selkoe, D.J., 1995. J. Biol. Chem. 270, 9564–9570.
Podlisny, M.B., Walsh, D.M., Amarante, P., Ostaszewski, B.L., Stimson, E.R., Maggio, J.E., Teplow, D.B., Selkoe, D.J., 1998. Biochemistry 37, 3602–3611.
Poling, A., Morgan-Paisley, K., Panos, J.J., Kim, E.M., O'Hare, E., Cleary, J.P., Lesne, S., Ashe, K.H., Porritt, M., Baker, L.E., 2008. Behav. Brain Res. 193, 230–234.
Pournaras, A.V., Koraki, T., Prodromidis, M.I., 2008. Anal. Chim. Acta 624, 301–307.
Resenberger, U.K., Harmeier, A., Woerner, A.C., Goodman, J.L., Muller, V., Krishnan, R., Vabulas, R.M., Kretzschmar, H.A., Lindquist, S., Hartl, F.U., et al., 2011. EMBO J. 30, 2057–2070.
Roychaudhuri, R., Yang, M., Hoshi, M.M., Teplow, D.B., 2009. J. Biol.Chem. 284, 4749–4753.
Rushworth, J.V., Griffiths, H.H., Watt, N.T., Hooper, N.M., 2013a. J. Biol. Chem..
Rushworth, J.V., Hirst, N.A., Goode, J.A., Pike, D.J., Ahmed, A., Millner, P.A., 2013b. Impedimetric biosensors for medical applications: current progress and challenges. ASME & Momentum Press, New York.
Rushworth, J.V., Hooper, N.M., 2010. Int. J. Alzheimers Dis. 2011, 603052.
Sakono, M., Zako, T., 2010. FEBS J. 277, 1348–1358.
Santos, A.N., Ewers, M., Minthon, L., Simm, A., Silber, R.-E., Blennow, K., Prvulovic, D., Hansson, O., Hampel, H., 2012. J. Alzheimers Dis. 29, 171–176.
Shankar, G.M., Bloodgood, B.L., Townsend, M., Walsh, D.M., Selkoe, D.J., Sabatini, B. L., 2007. J. Neurosci. 27, 2866–2875.
Shankar, G.M., Li, S., Mehta, T.H., Garcia-Munoz, A., Shepardson, N.E., Smith, I., Brett, F.M., Farrell, M.A., Rowan, M.J., Lemere, C.A., et al., 2008. Nat. Med. 14, 837–842.
Stravalaci, M., Bastone, A., Beeg, M., Cagnotto, A., Colombo, L., Di Fede, G., Tagliavini, F., Cantu, L., Del Favero, E., Mazzanti, M., et al., 2012. J. Biol. Chem. 287, 27796–27805.
Tomic, J.L., Pensalfini, A., Head, E., Glabe, C.G., 2009. Neurobiol. Dis. 35, 352–358.
Tsekenis, G., Garifallou, G.Z., Davis, F., Millner, P.A., Pinacho, D.G., Sanchez-Baeza, F., Marco, M.P., Gibson, T.D., Higson, S.P., 2008. Anal. Chem. 80, 9233–9239.
Um, J.W., Nygaard, H.B., Heiss, J.K., Kostylev, M.A., Stagi, M., Vortmeyer, A., Wisniewski, T., Gunther, E.C., Strittmatter, S.M., 2012. Nat. Neurosci. 15, 1227–1235.
Vardy, E.R., Catto, A.J., Hooper, N.M., 2005. Trends Mol. Med. 11, 464–472.
Walsh, D.M., Klyubin, I., Fadeeva, J.V., Cullen, W.K., Anwyl, R., Wolfe, M.S., Rowan, M. J., Selkoe, D.J., 2002. Nature 416, 535–539.
Walsh, D.M., Selkoe, D.J., 2007. J. Neurochem. 101, 1172–1184.
Wang-Dietrich, L., Funke, S.A., Kühbach, K., Wang, K., Besmehn, A., Willbold, S., Cinar, Y., Bannach, O., Birkmann, E., Willbold, D., 2013. J. Alzheimers Dis. 34, 985–994.
Wang, Q., Walsh, D.M., Rowan, M.J., Selkoe, D.J., Anwyl, R., 2004. J. Neurosci. *24*, 3370–3378.
Wesson, D.W., Levy, E., Nixon, R.A., Wilson, D.A., 2010. J. Neurosci. 30, 505–514.
Whitehouse, I.J., Jackson, C., Turner, A.J., Hooper, N.M., 2010. J. Alzheimers Dis. 22, 1023–1031.
Wimo, A., Prince, M., 2010. World Alzheimer Report 2010 – The Global Economic Impact of Dementia. Alzheimer's Disease International (ADI)London.
Yang, T., Hong, S., O'Malley, T., Sperling, R.A., Walsh, D.M., Selkoe, D.J., 2013. Alzheimers Dement. 9, 99–112.
Zhang, J.K., Wu, Y., Zhang, B.B., Li, M., Jia, S.R., Jiang, S.H., Zhou, H., Zhang, Y., Zhang, C.Z., Turner, A.P.F., 2012. Anal. Lett. 45, 986–992.
Zhou, L., Chan, K.H., Chu, L.W., Kwan, J.S.C., Song, Y.Q., Chen, L.H., Ho, P.W.L., Cheng, O.Y., Ho, J.W.M., Lam, K.S.L., 2012. Biochem. Biophys. Res. Commun. 423, 697–702.